

RESEARCH

Open Access



Antidepressant effect of *Radix bupleuri* - *Radix paeoniae alba* herb pair on chronic unpredictable mild stress rats based on cortical metabolomics

Kanglin Cai^{1,3†}, Xinyu Chen^{2,4†}, Yongkai Cao⁵, Liangdi Ran¹, Qinpeng Bu³, Dajun Hu¹, Zhitao Feng^{3*} and Meiqun Cao^{4,5*}

Abstract

Objective Depression is a serious mental disorder, and its incidence rate has increased rapidly. *Radix Bupleuri* (root of *Bupleurum chinensis* DC. BR)-*Radix Paeoniae Alba* (root of *Paeonia lactiflora* Pall. PRA) herb pair has been historically used for treating depression in Traditional Chinese Medicine (TCM) while the mechanisms need to be fully revealed.

Methods The effects of the BR-PRA herb pair were investigated using a rat model of chronic unpredictable mild stress (CUMS). First, the depressive-like behavior of rats was evaluated by open field test (OFT), elevated plus-maze test (EMP), and forced swimming test (FST). Secondly, histomorphological changes in the CA1 and CA3 regions of the hippocampus were analyzed by hematoxylin-eosin, nissl, and Golgi staining. Ultra high-performance liquid chromatograph tandem quadrupole mass spectrometry (UHPLC-QTRAP-MS/MS) was performed to reveal potential antidepressant mechanisms.

Results Following CUMS exposure, rats displayed depressive-like behavior, and neuronal death in the hippocampal region was observed. Consequently, these abnormal changes were reversed by BR-PRA herb-pair intervention. A total of 26 different metabolites related to depression were identified by metabolomics, mainly involving eleven metabolic pathways of pentose phosphate pathway, purine metabolism, and amino sugar and nucleotide sugar metabolism. BR-PRA herb-pair improved four metabolites, including homocitrulline, *N*-acetyllysine, corticosterone, and *N*-acetylglutamate. It also may affect the development of depression by interfering with the hypothalamus-pituitary-adrenal axis (HPA axis), amino acid metabolism related to lysine and glutamate, and modulation of oxidative stress.

[†]Kanglin Cai and Xinyu Chen contributed equally. contributed equally to this work.

*Correspondence:
Zhitao Feng
fengzhitao2008@126.com
Meiqun Cao
mqcao111@163.com

Full list of author information is available at the end of the article



© The Author(s) 2025. **Open Access** This article is licensed under a Creative Commons Attribution-NonCommercial-NoDerivatives 4.0 International License, which permits any non-commercial use, sharing, distribution and reproduction in any medium or format, as long as you give appropriate credit to the original author(s) and the source, provide a link to the Creative Commons licence, and indicate if you modified the licensed material. You do not have permission under this licence to share adapted material derived from this article or parts of it. The images or other third party material in this article are included in the article's Creative Commons licence, unless indicated otherwise in a credit line to the material. If material is not included in the article's Creative Commons licence and your intended use is not permitted by statutory regulation or exceeds the permitted use, you will need to obtain permission directly from the copyright holder. To view a copy of this licence, visit <http://creativecommons.org/licenses/by-nc-nd/4.0/>.

Conclusion BR-PRA herb-pair alleviated depressive-like behavior in CUMS rats, recovered hippocampus damage, and regulated cerebral cortex metabolism, which may be related to the HPA axis, amino acid metabolism related to lysine and glutamate, and modulation of oxidative stress.

Clinical trial number Not applicable.

Graphical Abstract

Keywords *Radix bupleuri*, *Radix paeoniae alba*, BR-PRA, Herb-pair, Depression, CUMS, Metabolomics

Introduction

Depression is a prevalent mental disorder characterized by significant and persistent depressed mood, with a high recurrence rate and a high suicide rate. According to the World Health Organization, about 350 million people worldwide suffer from depression, which is projected to become the leading cause of the global disease burden by 2030 [1]. Additionally, depression is a primary contributor to global disability, resulting in an ongoing increase in suicide prevalence [2, 3]. Current antidepressant drugs, however, displayed limited efficacy, long drug cycles, and poor patient compliance, resulting in unsatisfactory treatment effects of depression. A cross-sectional epidemiological survey conducted in China on a large scale revealed that a mere 0.5% of patients diagnosed with depression receive adequate treatment [4].

Traditional Chinese Medicine (TCM) has long been used for treating depression and has thus formed a relatively systematic theoretical understanding and valuable experience in diagnosis and treatment. Traditional Chinese antidepressant medicine is characterized by multi-components, multi-pathways, multi-targets, stable efficacy, overall regulation, and little toxicity, which has become a hot area of drug research [5]. In addition, herb-pair is the key component of traditional Chinese antidepressant medicine prescription, with the in-depth development of single medicine, and the beginning of compound medicine research. Therefore, research on TCM herb-pair medicine may provide new insights into antidepressant drugs.

Radix Bupleuri (the root of *Bupleurum chinensis* DC. BR) and *Radix Paeoniae Alba* (the root of *Paeonia lactiflora* Pall. PRA) were initially recorded in Shennong Bencao Jing in 200 AD. BR-PRA is a basic herb-pair and plays a dominant role in several commonly used and effective antidepressant prescriptions such as Xiaoyao San, Chaihu Shugan San, and Sini San [6, 7]. BR-PRA demonstrates a substantial potential for mitigating depression. As the most elementary and ubiquitously utilized antidepressant herbal medicine, their therapeutic efficacies have been substantiated [8, 9]. Specifically, the efficacy of *Radix Bupleuri* and *Radix Paeoniae Alba* in decreasing Hamilton Depression Rating Scale (HDRS) scores in individuals afflicted with depression is consistent with

that of conventional antidepressants, with fewer negative side effects [10], and also attenuates depression-like behaviors in various animal models of depression [11–13]. BR-PRA is supposed to regulate monoamine transmitters in different brain regions, including increasing the concentration of norepinephrine, dopamine, and serotonin, while reducing 5-hydroxyindole-3-acetic acid [11, 14], thereby attenuating depression. Inflammation is recognized as a significant pathway in the etiopathogenesis of depression, and recent research has indicated that BR-PRA can modulate inflammation and oxidative stress responses via various mechanisms [13, 15, 16]. Brain-derived neurotrophic Factor (BDNF) is one of the principal neurotrophic factors, which plays an important role in maintaining the structure and function of neuronal cell bodies and synapses [17]. Studies demonstrated that BR-PRA alleviated depressive behaviors by regulating BDNF expression [15, 18]. Moreover, the antidepressant effect of BR-PRA may be related to neuroplasticity, immune response, regulation of the HPA axis and energy metabolism, inhibition of neurotoxicity, and neuroprotection [7, 19]. However, the implications of BR-PRA on the hippocampus of CUMS rats and its mechanism of antidepressant effect have not been fully elucidated.

The cerebral cortex is the key part of the brain and participates in value judgment and decision-making, which is closely related to depression [16, 20]. The hippocampus is a brain region responsible for learning, memory, and emotional regulation. Its damage has led to psychological disorders such as anxiety and depression [21]. Chronic unpredictable mild stress (CUMS) is currently the most commonly used, reliable, and effective rodent model of depression [22]. Neurogenesis is a process in which neural stem cells gradually migrate to functional areas, continuously change plasticity, and establish connections with other neurons. In depression caused by CUMS, the volume of the cerebral cortex and hippocampus decreases, and dendritic atrophy and spine loss in neurons, contribute to the weakening of neurogenesis [23, 24].

Metabolomics, which is the profiling of metabolites category, quantity, and change regulation, is routinely applied as a tool for biomarker discovery. Widely targeted metabolomics, which combines the advantages

of the detection of non-targeted metabolomics and the accuracy of targeted metabolomics, has been applied to explore the efficacy and mechanism of TCM [25, 26]. Previous reports suggested synergies between different metabolomic methods [13]. However, there is a lack of widely targeted metabolomics research on depression, as indicated by recent literature reviews. This study, for the first time from a pathology perspective, clarified that BR-PRA reversed damage to neurons and dendritic spines in the hippocampus region of depression. Ultra High-performance Liquid Chromatograph Tandem Quadrupole Mass Spectrometry (UHPLC-QTRAP-MS/MS) cortex widely targeted metabolomics was used to explore the synergistic antidepressant effect of BR-PRA on CUMS rats and revealed the potential mechanism at the level of the metabolite.

Materials and methods

Animals

All adult male Sprague-Dawley (SD) rats (6–8-week-old, 200 ± 20 g) were purchased from the Experimental Animal Center of China Three Gorges University. Licences no. SCXK (E) 2017-0061. The experimental protocol was performed in compliance with the Animal Research: Reporting of In Vivo Experiments (ARRIVE) guidelines and was approved by the Ethical Committee in Research Medical College of China Three Gorges University of Medical Sciences (NO: 2023010U). All rats were kept under standard laboratory conditions (temperature: 20–24 °C, 12 h light/dark cycle: lights on 07:00–19:00, relative humidity: 45–55%), and free access to filtered water and standard food.

Chemicals and reagents

Radix Bupleuri and *Radix Paeoniae Alba* were acquired from Yichang Central People's Hospital. Fluoxetine hydrochloride was acquired from Eli Lilly Pharmaceutical Co., Ltd, Suzhou. Acetonitrile (Merck, 1499230-935), Methanol (Fisher, A456-4), formic acid (Sigma, 00940), Ammonium formate (Sigma, 70221), Ammonium acetate (Sigma, 73594) was used for UHPLC-QTRAP-MS/MS.

Drug Preparation

Fluoxetine hydrochloride was prepared by dissolving in deionized water at a rate of 0.2 mg/ml. *Radix Bupleuri* (0.5 kg) and *Radix Paeoniae Alba* (0.5 kg) were immersed in 70% ethanol (1:8, w/v) twice for 1.5 h each time. Then herb-pair was filtrated and concentrated in vacuo lyophilized into powders and stored at 4 °C refrigerator. The extraction rate of BR-PRA is 15.23%. The configured concentrations of the high-dose BR-PRA group and the low-dose BR-PRA group were 0.228 g/ml and 0.114 g/ml, respectively, for animal experiments. HERB database (<http://herb.ac.cn/>) [27] and TCMSP database (<https://old.tcmsp-e.com/tcmsp.php>) [28] are unique pharmacological platforms in the traditional Chinese medicine system, recording the identified active compounds of traditional Chinese medicines. This study compared all active ingredients obtained through high-performance liquid chromatography identification with the identified ingredients in traditional Chinese medicine databases HERB database and TCMSP database, and finally included them (Figure S1, Table S1). These compounds can all be found in the HERB and TCMSP databases.

Chronic unpredictable mild stress procedure

Rats were randomly divided into 5 groups: control group, CUMS group, low-dose BR-PRA group, high-dose BR-PRA group, and fluoxetine group (positive group). Each group contained 6 rats. Except for the control group, all other groups were randomly given daily stimuli including fasting for 24 h, water cut-off for 24 h, tail clipping for 2 min, swimming in 4 °C ice water for 5 min, day and night reversal, 45° cage tilting, binding, and wet padding [29], and so on within 28 days. The flow chart of the depression model is shown in Fig. 1. All the rats were fed normally. From the 15th day, the control and model group was given sterile distilled water, the low-dose group was given BR-PRA 7.5 g/kg, the high-dose group was given BR-PRA 15 g/kg [13], and the positive control group was given fluoxetine 2 mg/kg [29]. All rats were given 10 ml/kg body weight by gavage once a day until the 28th day.

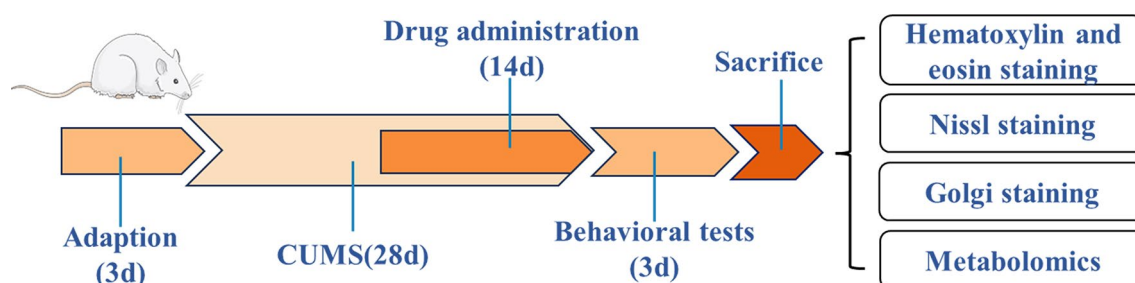


Fig. 1 Experimental procedure design. The behavioral tests of rats were evaluated using the Open field test (OFT), the Elevated plus-maze (EPM) test, and the Forced swimming test (FST)

Behavioral tests

After 28 days of CUMS exposure, behavioral changes in the rats were recorded using Xinsoft camera equipment (Shanghai Xinsoft Information Technology Co., Ltd.). The assessments were performed using three tests: open field test (OFT) [30], elevated plus-maze (EPM) test [29], and forced swimming test (FST) [16] in succession with minor modifications.

Sample collection

After the last behavioral test, all rats were anesthetized by intraperitoneal injection of pentobarbital sodium (50 mg/kg), and euthanized by decapitation when the rats lost consciousness [31], thus rapidly isolating the entire brain. The left hemisphere was removed and fixed with 4% paraformaldehyde, and the right hippocampus and cerebral cortex were separated and immediately stored at -80°C .

Hematoxylin and eosin(H&E) and Nissl staining

the hippocampus of each rat was used for histopathological examination, and the procedure and evaluation criteria were the same as previously described [29]. Quantitation of Nissl staining neurons of the hippocampus was observed at a magnification of 200 \times .

Golgi staining

The hippocampi were fixed to 4% paraformaldehyde (Servicebio, G1101) for 48 h. and cut into 2–3 mm slides. The obtained tissue slices were completely immersed in Golgi solution and kept in the dark for 14 days (replacing Golgi solution after 48 h, then changing to a new dye solution every 3 days). After being maintained in 80% glacial acetic acid solution overnight, and dehydrated in 30% sucrose solution, brain tissue was cut into 100 microns by an oscillating microtome and made into gelatin slices for overnight drying in darkness. The sections were treated with ammonium hydroxide for 15 min, distilled water for 1 min, and fixed bath for 15 min, and then sealed with glycerol gelatin. The density of dendritic spines was assessed utilizing optical microscopy (NIKON, Japan). The number of dendritic spines present in neurons located within the hippocampal region of rats across each experimental group was recorded for subsequent quantitative analysis.

Cortex metabolomics analysis

Based on the results of behavioral tests and histomorphological analysis, low-dose administration of BR-PRA was found to be more effective, consistent with prior reports [16]. Consequently, cortical samples were collected from the control group, model group, low-dose BR-PRA group, and fluoxetine group for metabolomics analysis. The original data of cortical metabolites were obtained

by coupling the ultrahigh performance liquid chromatograph (1290 Infinity LC, Agilent Technologies) of Shanghai Applied Protein Technology Co., Ltd. with QTRAP MS (6500+, Sciex). Normalization data was imported into *SIMCA-P* (version 14.1, Umetrics, Umea, Sweden) to obtain differential metabolites. Further details can be found in the Supplementary material. The differential metabolites obtained were imported into the database *MetaboAnalyst 6.0* for enrichment analysis.

Statistical analysis

Statistical analysis was performed using *SPSS 22.0* software (Chicago, IL, USA). Data were expressed as mean \pm standard deviation. Normal distribution data were compared between two groups using the independent sample *t*-test and three or more groups were compared using the one-way analyses of variance (ANOVA) test. Pairwise comparisons were made using the least significant difference (LSD) post-hoc test after one-way ANOVA. The non-parametric Kruskal-Wallis test was used to analyze non-normal distribution data. The statistical significance was set at $P < 0.05$.

Result

BR-PRA improved behavioral changes in chronic unpredictable mild stress rats

Representative tracks from the OFT are shown in Fig. 2A. Exposure to Chronic Unpredictable Mild Stress (CUMS) led to a significant decrease in total moving distance compared to the control group (Fig. 2C, $P < 0.05$). Treatment with low and high doses of BR-PRA resulted in a significant increase in total moving distance compared to the CUMS group (Fig. 2C, $P < 0.01$). Fluoxetine also improved the total moving distance of the rats (Fig. 2C, $P < 0.05$). As illustrated in Fig. 2D, rats in the Model group exhibited significantly fewer rearing times in the open field compared to the control group ($P < 0.01$). All drug intervention groups demonstrated a significant increase in rearing times compared to the Model group.

Representative tracks from the EMP test are shown in Fig. 2B. Figure 2E shows that rats in the CUMS group had a significantly shorter time to enter the open arm compared to the control group. In contrast, the low and high-dose BR-PRA groups took significantly longer to enter the open arm compared to the Model group, and there was a trend toward improvement observed in the fluoxetine group. However, the experiment found no significant differences in the number of entries into the open arm following CUMS stimulation.

Figure 2G indicates that the duration of immobility in the CUMS group was significantly increased compared to the control group ($P < 0.01$). Conversely, administration of BR-PRA in both low and high doses significantly

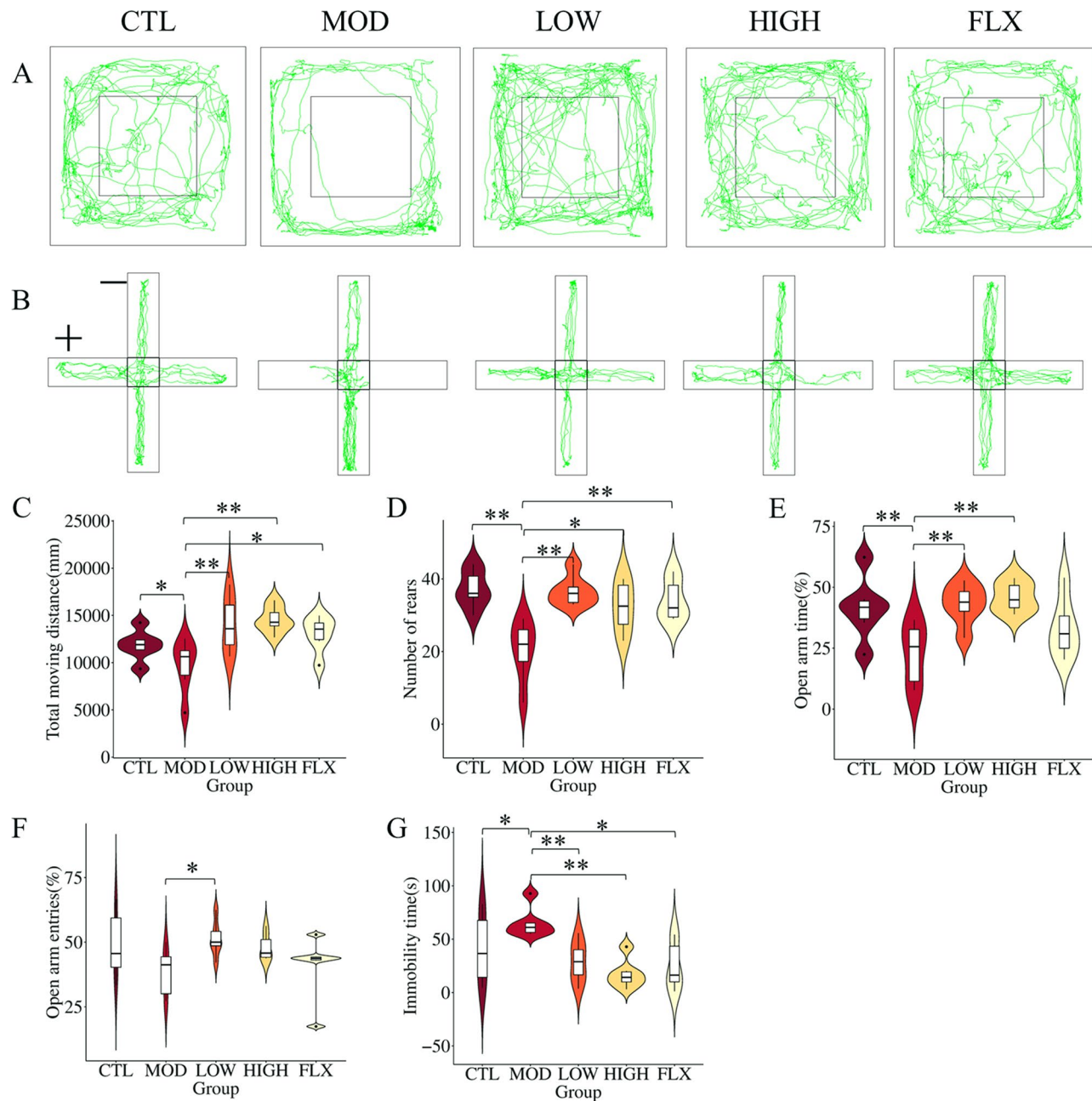


Fig. 2 Behavioral test of rats with chronic unpredictable depression ($n=6$); **(A)**: Representative images of open field test (OFT); **(B)**: Representative images of elevated plus-maze (EPM; Open arm, -: enclosed arm, the middle is the central area) test; **(C)**: Total moving distance of rats in the open field; **(D)**: Rearing times of rats in the open field; **(E)**: Open arm time of rats in the elevated plus-maze (%); **(F)**: Open arm entries of rats in the elevated plus-maze (%); **(G)**: Rats immobility time in water; CTL: Control group; MOD: Model group; LOW: *Radix Bupleuri-Radix Paeoniae Alba* at low dose group; HIGH: *Radix Bupleuri-Radix Paeoniae Alba* at high dose group; FLX: Fluoxetine group; * $P < 0.05$, ** $P < 0.01$

reduced the duration of immobility compared to the Model group ($P < 0.05$, $P < 0.01$).

These results confirm that the depressed model was successfully established. BR-PRA significantly reversed depression-like behavior in rats, with efficacy equivalent to the positive drug fluoxetine.

BR-PRA improved histomorphology changes in chronic unpredictable mild stress rats

Figures 3A-D show representative H&E staining images. In the control group, neurons in the CA1 and CA3 hippocampus regions were arranged closely and neatly, completely structured, and the cell nucleus was clear and full. However, neurons in the model group are necrotic, loose, and disordered, with atrophy or swelling and a lack of a

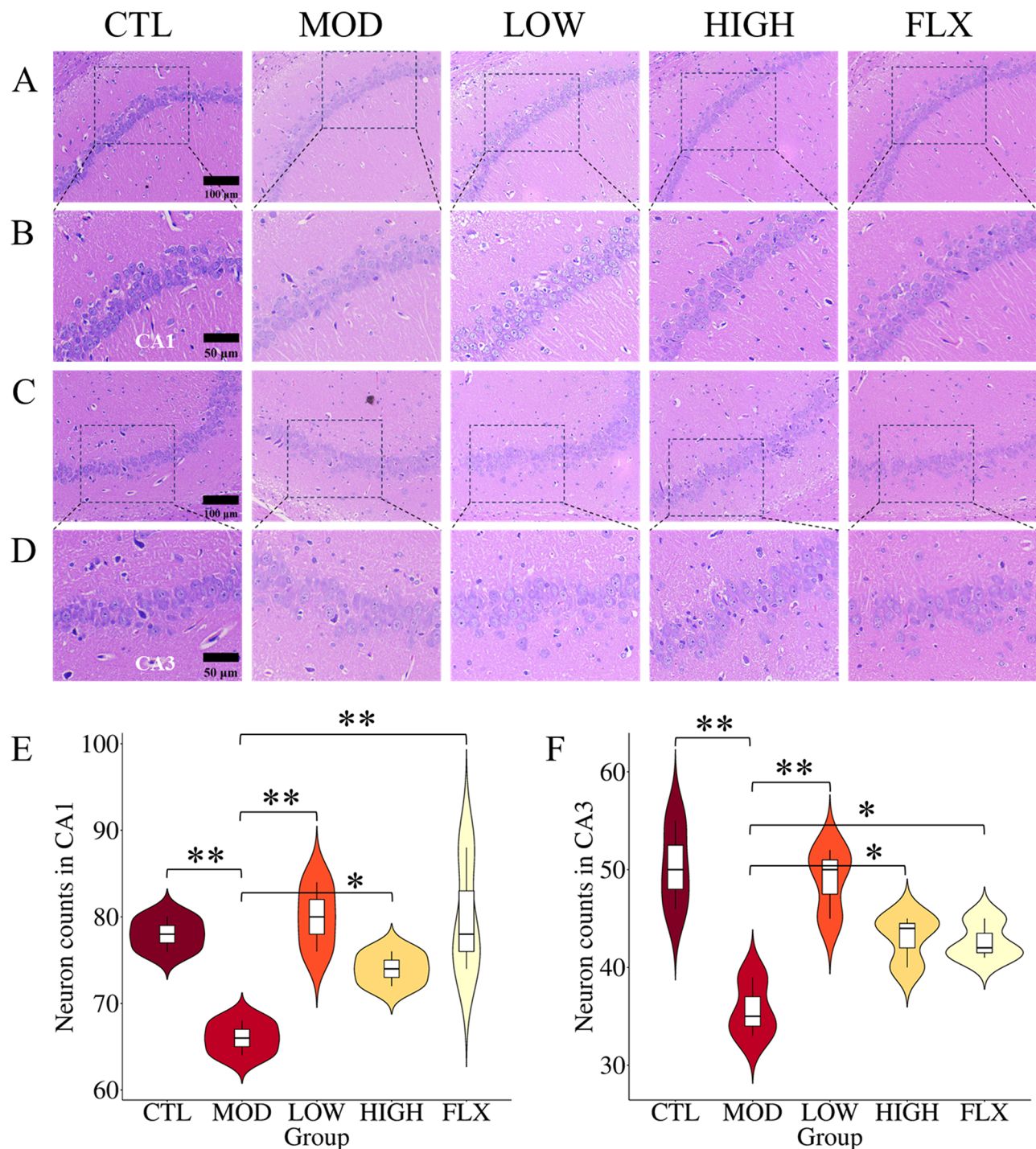


Fig. 3 Representative images of Hematoxylin and eosin (H&E) staining in the hippocampal region, (A, C): 200× magnification, scale bar = 100 μm, (B, D): 400× magnification, scale bar = 50 μm; (E, F): Quantification of the neurons of CA1 and CA3 region ($n = 3$), Neurons with visible nuclei, distinctive nucleolus, and cytoplasmic Nissl staining were regarded as intact neurons and counted; CTL: Control group; MOD: Model group; LOW: *Radix Bupleuri-Radix Paeoniae Alba* at low dose group; HIGH: *Radix Bupleuri-Radix Paeoniae Alba* at high dose group; FLX: Fluoxetine group; * $P < 0.05$, ** $P < 0.01$

nucleus, and decreased normal neurons ($P < 0.01$, Fig. 3E and F). Compared with the model group, the above conditions reversed to varying degrees after all drug interventions, and increased normal neurons ($P < 0.05$, $P < 0.01$, Fig. 3E and F).

Representative images of Nissl staining are presented in Figs. 4A-D. Analysis of the Nissl staining in the hippocampal regions CA1 and CA3 of rats subjected to CUMS revealed significant abnormalities, including degeneration and necrosis, incomplete stratification, irregular

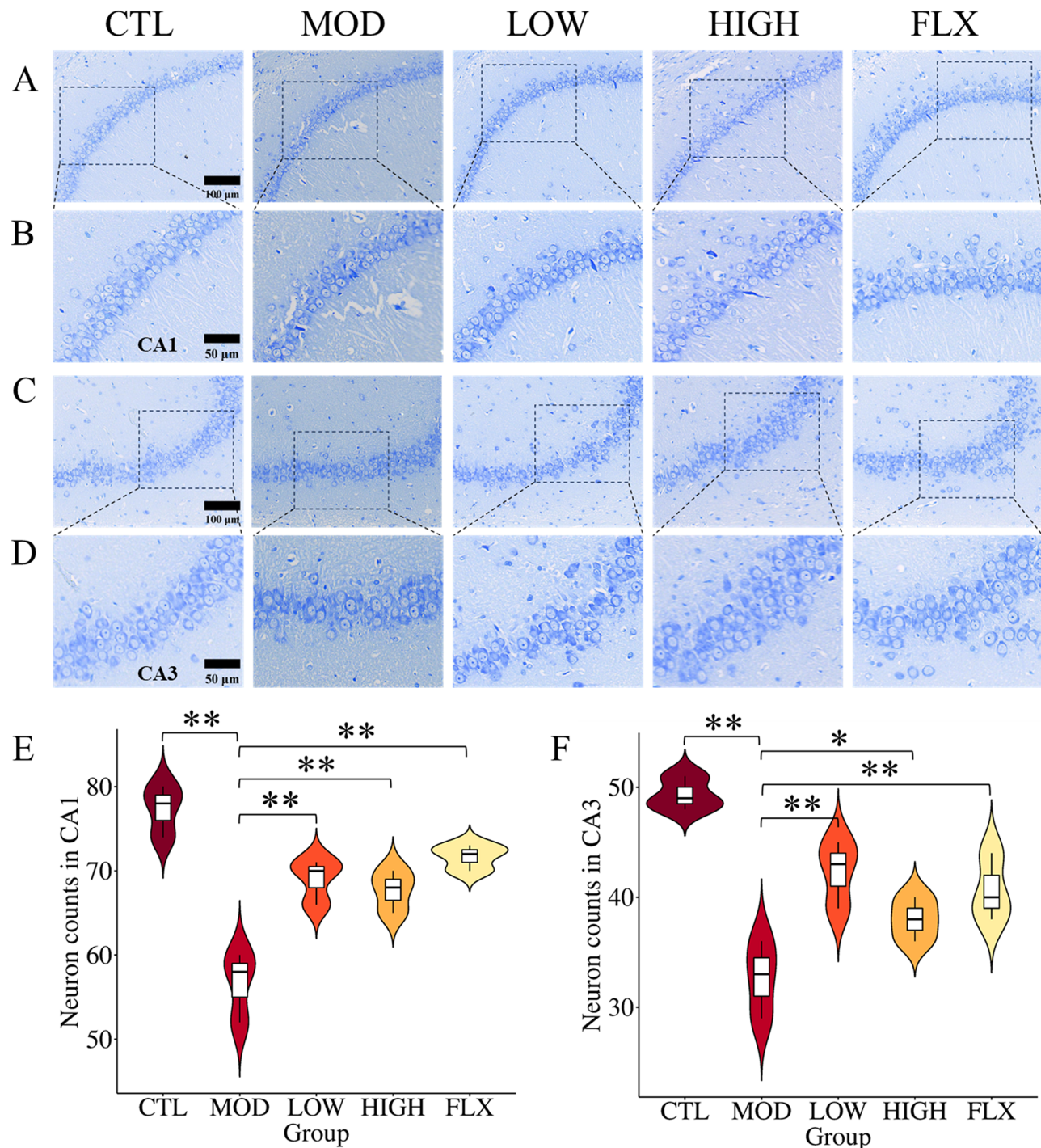


Fig. 4 Representative images of Nissl staining in the hippocampal region, (A, C): 200× magnification, scale bar = 100 μm, (B, D): 400× magnification, scale bar = 50 μm; (E, F): Quantification of the neurons of CA1 and CA3 region ($n=3$), Neurons with visible nuclei, distinctive nucleolus, and cytoplasmic Nissl staining were regarded as intact neurons and counted; CTL: Control group; MOD: Model group; LOW: *Radix Bupleuri-Radix Paeoniae Alba* at low dose group; HIGH: *Radix Bupleuri-Radix Paeoniae Alba* at high dose group; FLX: Fluoxetine group; * $P < 0.05$, ** $P < 0.01$

neuronal arrangement, the presence of Nissl bodies, and a decrease in normal neurons ($P < 0.01$, Fig. 4E and F). In comparison to the model group, all drug intervention groups displayed a tighter neuronal arrangement, reduced necrosis and Nissl bodies, and an increased

number of normal neurons ($P < 0.05$, $P < 0.01$, Fig. 4E and F).

Representative Golgi staining images are demonstrated in Fig. 5A and B. The morphology of dendritic spines greatly influences the functionality of synaptic

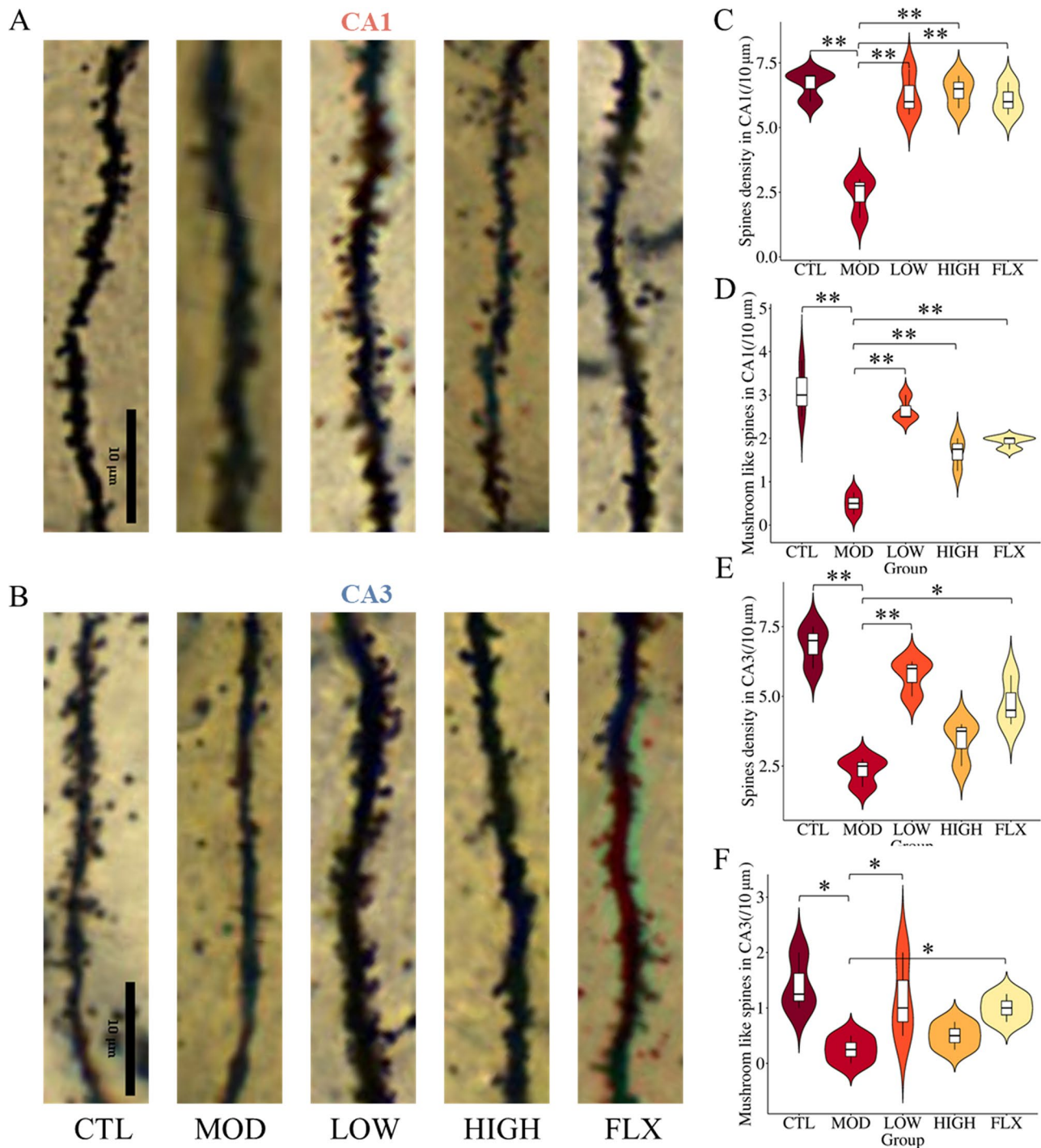


Fig. 5 Representative images of Golgi staining in hippocampal region, (A, B): 1200× magnification, scale bar = 10 μm; (C–F): Quantification of the density of total spines and mushroom-like spines ($n=3$); CTL: Control group; MOD: Model group; LOW: *Radix Bupleuri-Radix Paeoniae Alba* at low dose group; HIGH: *Radix Bupleuri-Radix Paeoniae Alba* at high dose group; FLX: Fluoxetine group; * $P < 0.05$, ** $P < 0.01$

connections. Mushroom-like spines are typically indicative of functional synapses, while rod-shaped and stubby spines often indicate an absence of functional synapses. To fully understand the structure and function of the hippocampus, Golgi staining techniques were employed to examine and quantify the complexity of dendritic spines,

specifically focusing on the presence and abundance of mushroom-like spines. As illustrated in Fig. 5C and F, the density of total dendritic spines and mushroom-like dendritic spines in the hippocampal CA1 region of the model group notably decreased, exhibiting a significant improvement following drug intervention ($P < 0.01$). It

is noteworthy to highlight that in the CA3 region, only the low-dose BR-PRA group and fluoxetine group were capable of reversing the decline in total spine density and mushroom spine density attributed to chronic unpredictable mild stress, and the high-dose BR-PRA group failed to ameliorate the spine density decline.

These results indicate that CUMS exposure causes damage to neurons and dendritic spines in the hippocampus of rats, and the effects of this damage can be significantly mitigated by BR-PRA administration. Among them, the effect of the low-dose BR-PRA group is superior to the high-dose BR-PRA group, and its effect is equivalent to the positive drug fluoxetine.

Metabolites and metabolic pathway analysis revealed the effect of BR-PRA in chronic unpredictable mild stress rats

Multivariate data analysis

In the PCA model, there was a tendency between the CUMS group and the control group, and QC samples were closely clustered, indicating that the samples were stable and had good repeatability (Fig. 6A). In the OPLS-DA model, R^2_X , R^2_Y , and Q^2 were 0.406, 0.999, and 0.658 respectively, which showed that the OPLS-DA model was successfully established, and the control group and the model group were significantly separated (Fig. 6B). The permutation test was used to validate the OPLS-DA model (Fig. 6C). The t-test variable ($P < 0.05$) combined with $VIP > 1$ (Fig. 6D) was used to determine various depression metabolites. Furthermore, in the OPLS-DA model (Fig. 6E), the BR-PRA and control groups showed some level of differentiation, and the normal and fluoxetine groups were different from the model group.

Differential metabolites analysis

Changes in cortical metabolites were detected in rats exposed to CUMS. A total of 26 different metabolites were screened ($VIP > 1.0$ and $P < 0.05$). The differential metabolites associated with depression are shown in Table 1; Fig. 7A. Compared with the control group, 15 differential metabolites, *N*-alpha-acetyllysine, *N*-acetylglutamic acid, homocitrulline, etc. were significantly increased, 11 differential metabolites, hydroxyproline, glycerol-myristate, palmitoylethanolamide, etc. were significantly decreased in model group. Among them, differential metabolites associated with depression included 7 carboxylic acids and derivatives, 6 steroids and steroid derivatives, 5 organooxygen compounds, 3 purine nucleotides, etc.

Compared with the model group, BR-PRA could regulate 4 metabolites including homocitrulline, *N*-alpha-acetyllysine, corticosterone, and *N*-acetylglutamic acid. Furthermore, acetylcholine, arachidonoyl ethanolamide, *N*-methyl-aspartic acid, linoleoyl ethanolamide,

deoxyadenosine monophosphate, 3-methylhistidine, and hydoxycholeic acid (HDCA) also showed significant changes. There are 5 carboxylic acids and derivatives, 2 steroids and steroid derivatives, 2 organonitrogen compounds, 1 tetrapyrroles and derivatives, and 1 Pyridine nucleotides. Carboxylic acids and derivatives serve an integral role in the pathogenesis of depression, and the potential antidepressant efficacy of BR-PRA may be intimately linked to these compounds. Compared with the model group, fluoxetine could regulate 14 metabolites including indole-3-methyl acetate, *N*-alpha-acetyllysine, hydroxyproline, homocitrulline, etc.

To better comprehend the interrelationship between differential metabolites, correlation analysis was conducted to establish the degree of association between these metabolites. The correlation network of differential metabolites was shown in Fig. 7B (Pearson correlation coefficient $|r| > 0.8$, $P < 0.05$) [32], which obtained both direct and indirect connections between metabolites. Among them, mannose-6-phosphate, homocitrulline, 2-methylcitric Acid, *N*-acetylglutamic acid, and *N*-alpha-acetyllysine were the key nodes, indicating that 5 metabolites may play an important role in depression. In addition, there was a significant positive correlation between homocitrulline and *N*-alpha-acetyllysine, *N*-alpha-acetyllysine and *N*-acetylglutamic acid, β -UDCA and CDCA; *N*-acetylglutamic acid and β -UDCA, galactose 1-phosphate and palmitoylethanolamide, mannose 6-phosphate and palmitoylethanolamide had a significant negative correlation.

Pathway analysis

26 Differential metabolites associated with depression and 11 differential metabolites regulated by BR-PRA were imported into *Metaboanalyst 6.0* for metabolic pathway analysis. 11 depression-related metabolic pathways were found (Fig. 8A, C), showing pentose phosphate pathway, purine metabolism, amino sugar and nucleotide sugar metabolism, arginine biosynthesis, fructose and mannose metabolism, galactose metabolism, biosynthesis of unsaturated fatty acids, arginine and proline metabolism, pyrimidine metabolism, primary bile acid biosynthesis, steroid hormone biosynthesis. Arginine biosynthesis, Histidine metabolism, Glycerophospholipid metabolism, Purine metabolism, and Steroid hormone biosynthesis could be mediated by BR-PRA (Fig. 8B).

Discussion

In this study, the exploratory ability, spontaneous activity, exploratory desire, and despair response of CUMS rats were weakened, but BR-PRA intervention reversed depressive behavior. Evaluation of changes in hippocampal histomorphology showed a decrease in hippocampal neurons in the CA1 and CA3 regions of CUMS

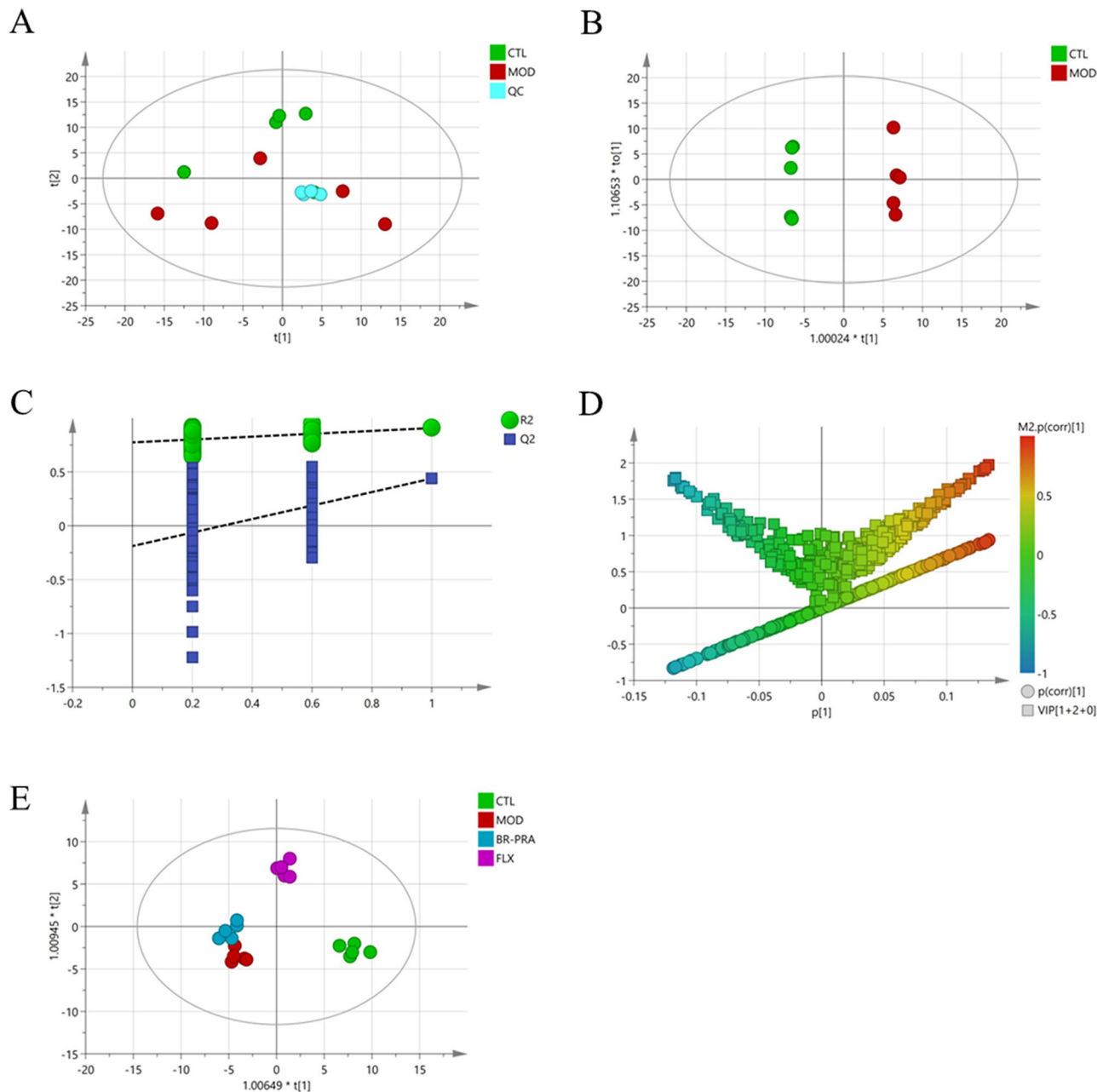


Fig. 6 Multivariate data analysis from UHPLC-QTRAP-MS/MS (n=5). **(A):** PCA scores of the control, model and quality control (QC) groups; **(B):** OPLS-DA scores of the control and model groups; **(C):** OPLS-DA model validation diagram; **(D):** V-S-plot; **(E):** OPLS-DA scores of the CTL, MOD, PA-PRA, FLX groups; CTL: Control group; MOD: Model group; BR-PRA: *Radix Bupleuri-Radix Paeoniae Alba* group; FLX: Fluoxetine group

rats, with abnormal cell integrity and morphology. Nissl bodies were significantly reduced, and the structure and complexity of neuronal dendrites were weakened. Compared with the model group, BR-PRA relieved the damage in the CA1 and CA3 regions of the hippocampus induced by CUMS. All these results indicate that BR-PRA exhibits an antidepressant effect. Furthermore, changes in cerebral cortex metabolites were identified by HPLC-QTRAP-MS/MS to determine the potential mechanism of BR-PRA for antidepressants. A total

of 26 depression-related differential metabolites were identified, with 4 metabolites (homocitrulline, N-alpha-acetyllysine, corticosterone, and N-acetylglutamic acid) regulated by BR-PRA.

Previous studies have indicated that Homocitrulline (*N*-ε-carbamyllysine) is a product of lysine carbamylation [33], while *N*-alpha-acetyllysine is a derivative of lysine acetylation. Furthermore, the conversion of Lysine to saccharopine through condensation with α-ketoglutarate by the enzyme L-lysine-ketoglutarate

Table 1 Differential metabolites associated with depression

Name	Class	HMDB	RT (min)	P value	VIP	Tread
N-alpha-acetyllysine	Carboxylic acids and derivatives	0000446	7.34	1.22E-05	2.6	↑
N-acetylglutamic acid	Carboxylic acids and derivatives	0001138	7.95	1.06E-04	2.52	↑
Homocitrulline	Carboxylic acids and derivatives	0000679	7.37	1.48E-04	2.5	↑
2-methylcitric Acid	Carboxylic acids and derivatives	0000379	9.09	0.0027	2.25	↑
Indole-3-methyl acetate	Indoles and derivatives	0029738	5.99	0.0046	2.2	↑
Hydroxyproline	Carboxylic acids and derivatives	0000725	6.5	0.0064	2.14	↓
Glycerol-myristate	Glycerolipids	0011561	10.5	0.0083	2.09	↓
Palmitoylethanolamide	Carboximidic acids and derivatives	0002100	11.03	0.0093	2.07	↓
Mannose 6-phosphate	Organooxygen compounds	0001078	9.08	0.0102	2.07	↑
Deoxycytidine	Organic oxoanionic compounds	0000014	2.5	0.0105	2.05	↓
Ursodeoxycholic acid (UDCA)	Steroids and steroid derivatives	0000946	8.54	0.0112	2.06	↓
Murocholic acid (MoCA)	Steroids and steroid derivatives	0000811	8.23	0.0126	2.02	↓
IDP	Purine nucleotides	0003335	9.46	0.0130	2	↑
Thyronine	Carboxylic acids and derivatives	0000667	8.39	0.0133	2.02	↓
Chenodeoxycholic acid (CDCA)	Steroids and steroid derivatives	0000518	8.54	0.0135	2.03	↓
Galactose 1-phosphate	Organooxygen compounds	0000645	9.42	0.0161	1.77	↑
Inosine-monophosphate	Purine nucleotides	0000175	8.99	0.0172	1.97	↑
Beta-ursodeoxycholic acid (β-UDCA)	Steroids and steroid derivatives	0000686	8.54	0.0183	1.96	↓
N-acetylneuraminic acid	Organooxygen compounds	0000230	7.38	0.0229	1.9	↑
Beta-hydoxycholic acid (β-HDCA)	Steroids and steroid derivatives	0000664	8.84	0.0258	1.89	↓
D-sedoheptulose 7-phosphate	Organooxygen compounds	0001068	9.7	0.0263	1.87	↑
ADPG	Purine nucleotides	0006557	8.75	0.0339	1.84	↑
Corticosterone	Steroids and steroid derivatives	0001547	6.96	0.0353	1.81	↑
Gamma-linolenic acid	Fatty Acyls	0003073	10.99	0.0454	1.78	↑
D-ribose 5-phosphate	Organooxygen compounds	0001548	8.97	0.0482	1.73	↑
Ricinoleic acid	Fatty Acyls	0034297	9.94	0.0478	1.71	↓

Note: Compared with the control group, “↑” the expression level is up-regulated; “↓” the expression level is down-regulated

reductase. Subsequently, the saccharopine is reduced to 2-aminoadipic semialdehyde by the action of saccharopine dehydrogenase, simultaneously liberating glutamate. The synthesis of N-acetylglutamic acid from glutamic acid and acetyl-CoA [34] is a key process in the initiation of arginine biosynthesis. Interestingly, arginine biosynthesis($P<0.05$) is significantly enriched in the anti-depressant pathway by the BR-PRA group. arginine and its metabolites play an important role in the development and persistence of depression [35]. Lysine serves as an essential precursor for de novo synthesis of glutamate, the most significant excitatory neurotransmitter in the mammalian central nervous system [36]. Therefore, homocitrulline, N-alpha-acetyllysine, and N-acetylglutamic acid are all derived from catabolism or post-translational modification of lysine. To further elucidate the relationship between differential metabolites, we conducted a correlation analysis, revealing a high correlation among mannose-6-phosphate, homocitrulline, 2-methylcitric acid, N-acetylglutamic acid, N-alpha-acetyllysine, palmitoylethanolamide, β-UDCA, ADPG, and D-Ribose 5-phosphate. Moreover, significant positive correlations were observed between homocitrulline and N-alpha-acetyllysine, N-alpha-acetyllysine and N-acetylglutamic acid, as well as β-UDCA and CDCA; N-Acetylglutamic

acid and β-UDCA. Conversely, Galactose 1-phosphate and palmitoylethanolamide, Mannose 6-phosphate, and palmitoylethanolamide exhibited significant negative correlations. Of particular note is the strong correlation between homocitrulline and N-alpha-acetyllysine, N-alpha-acetyllysine, as well as N-acetylglutamic acid (Coefficient > 0.8), indicating their connection and potential important role in depression.

Lysine (Lys) is an essential amino acid that plays a crucial role in mammalian brain function. Previous studies have demonstrated that L-lysine exhibits antidepressant and anti-anxiety effects. Animal research has shown that L-lysine may influence neurotransmitters involved in stress and anxiety, and L-lysine acts as a partial serotonin receptor 4 antagonist, leading to a decrease in the brain-gut response to stress and cortisol levels in the blood [37, 38]. In a placebo-controlled study investigating the effects of L-lysine-containing supplements in humans, it was found that a combination of L-lysine and L-arginine supplements improved participants' ability to handle induced stress by increasing cortisol levels [39, 40]. Recent studies have demonstrated that Lys and its metabolites modulate benzodiazepine and G-protein-coupled receptors in the central nervous system [41, 42]. Lys deficiency contributes to alterations in neurotransmitters

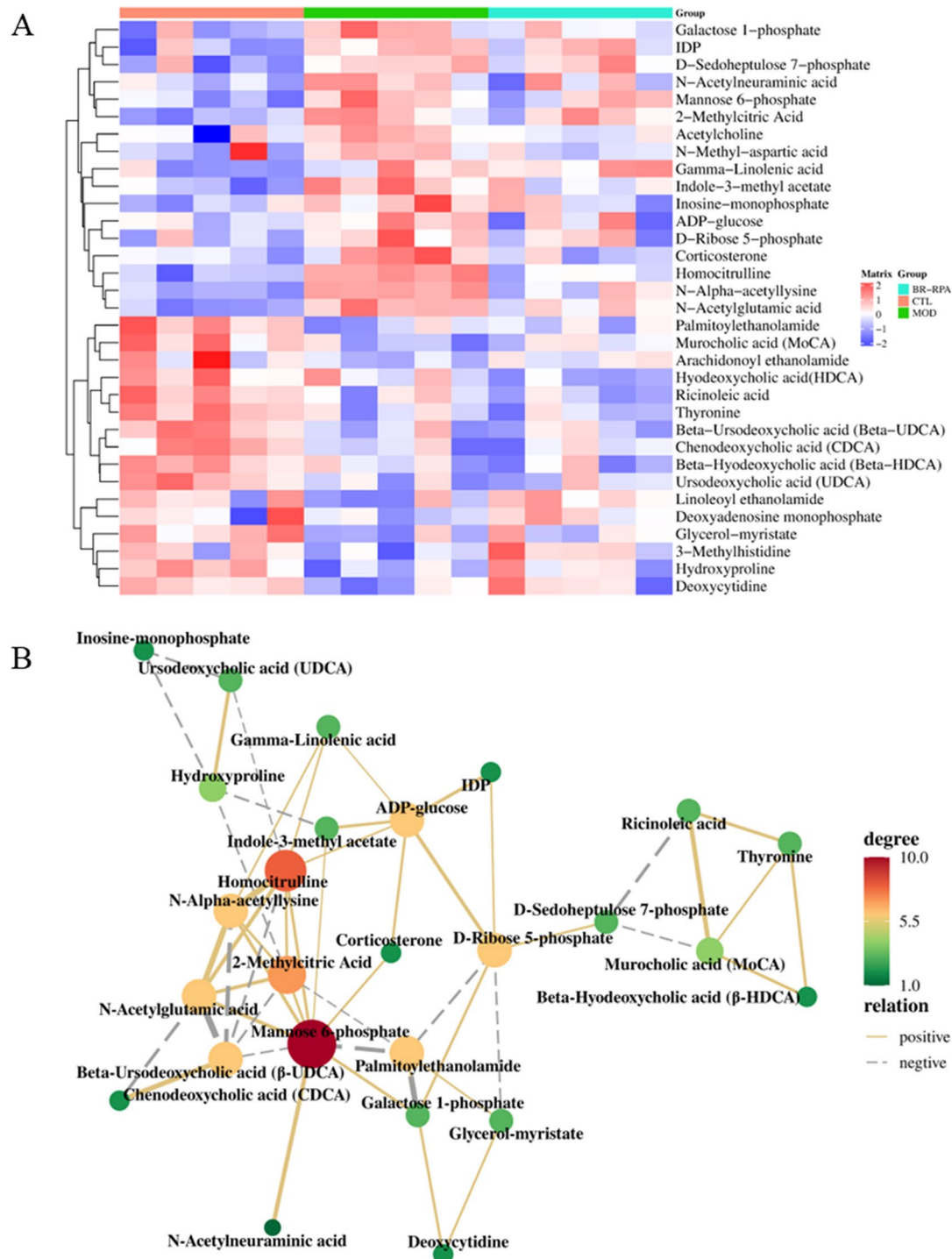


Fig. 7 **A:** Heat map of the differential metabolites. Red and blue indicate that the levels of differential metabolites are above and below average, respectively. Rows represent differential metabolites, and the list shows samples ($n = 5$); **B:** The correlation network of differential metabolites. The degree value represents the number of edges connected to the pointing node. Nodes represent the targets of differential metabolites, the greater the degree, the greater Node; Solid lines represent positive correlation, and dashed lines represent positive correlation, the thicker line, the greater correlation.CTL: Control group; MOD: Model group; BR-PRA: *Radix Bupleuri-Radix Paeoniae Alba* group

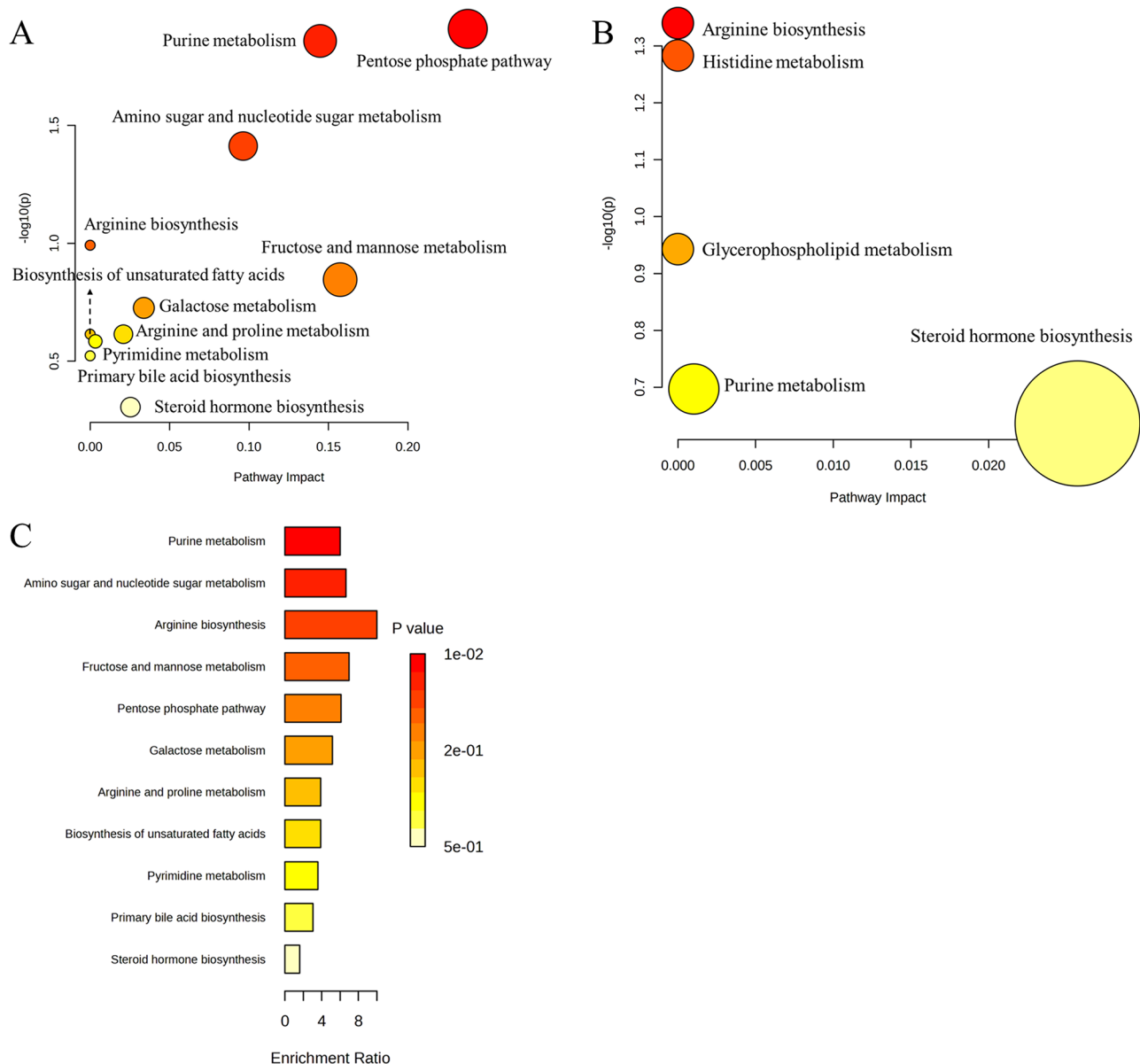
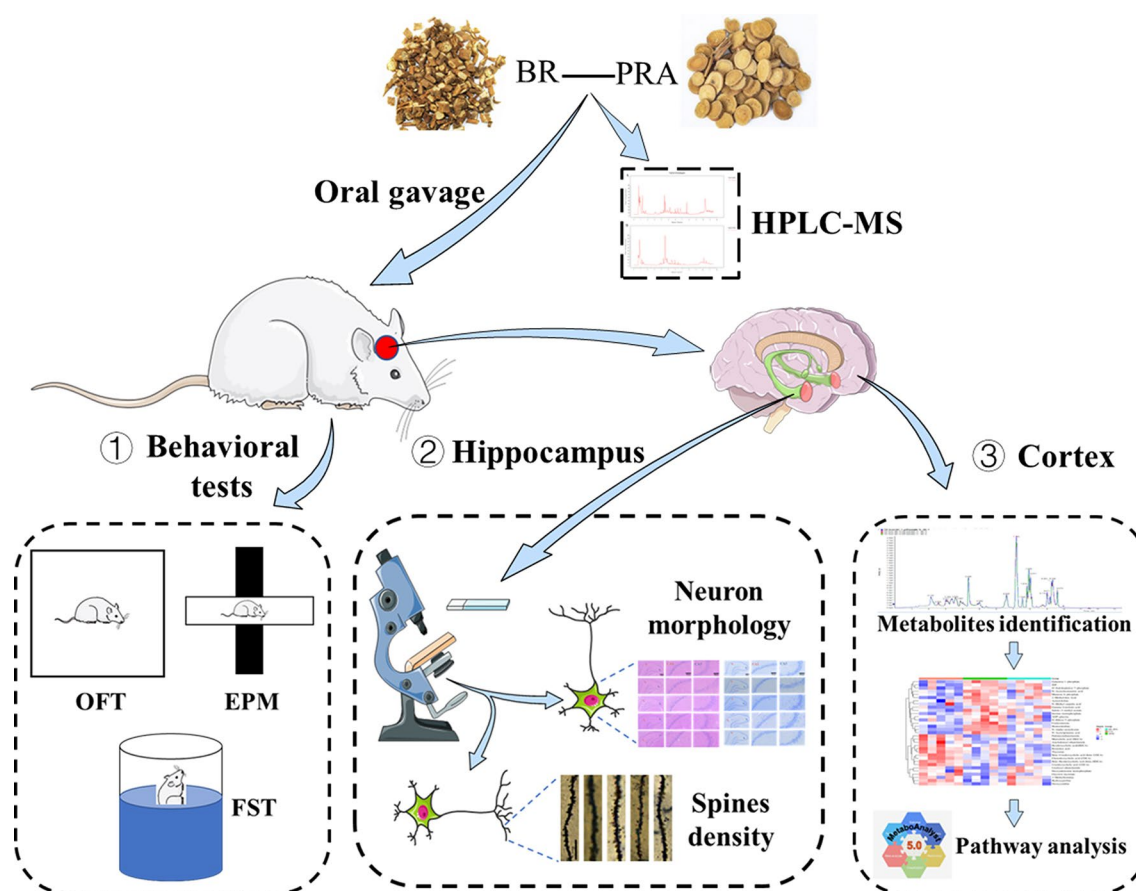


Fig. 8 Metabolic pathway analysis: **(A)** Control VS Model group. **(B)**: Model VS RA-RPA group. The magnitude of each node represents its pathway impact, and the darker shade of the node implies a more significant disparity. **(C)**: Enrichment analysis of differential metabolic pathways. Enrichment Ratio is computed by Hits / Expected, where hits = observed hits; expected = expected hits

such as noradrenaline and serotonin in the amygdala and hypothalamus [43, 44]. Furthermore, microiontophoretic experiments *in vivo* have shown that lysine completely blocks glutamate-evoked neuronal excitation, suggesting that lysine suppresses glutamatergic neuronal activity, thereby modulating brain activity [45]. Depression is closely related to changes in neurotransmitters such as glutamatergic, serotonergic, and GABAergic systems [46–48]. Therefore, lysine may exert modulatory actions on cellular physiological processes, such as cell proliferation, differentiation, excitability, and intercellular

interaction through neurotransmitter systems. It is also involved in the pathogenesis and treatment of depression.

On the other hand, lysine carbamylation and lysine acetylation are both post-translational modifications that have been proposed to mediate diverse environmental aspects involved in the pathophysiology of major psychotic disorders. Lysine acetylation and deacetylation represent prominent posttranslational modifications of histone tails that affect chromatin structure and epigenetic states, playing an essential role in brain development and function [49]. A postmortem investigation revealed that individuals with bipolar disorder exhibited



higher baseline levels of total acetylated histone 3 compared to those with schizophrenia [50]. Histone deacetylase inhibitors have demonstrated the ability to regulate epigenetic programming associated with cognition and behavior, and are considered a potential therapeutic target for mood disorders such as bipolar disorder and major depressive disorder [51].

Oxidative stress refers to the imbalance between oxidation and antioxidation [52]. Cellular oxidative stress occurs when an imbalance between the generation of ROS and antioxidant defenses causes irreparable oxidative damage. Protein lysine carbamylation is an irreversible post-translational modification resulting in the formation of homocitrulline (N- ϵ -carbamyllysine). Research has shown that intraventricular administration of homocitrulline affects glutathione (GSH) concentration and the activities of catalase (CAT) and glutathione peroxidase (GSH-Px) in the cerebral cortex, thereby reducing antioxidant capacity [53, 54]. It indicates that homocitrulline induces lipid peroxidation, most probably through the formation of reactive oxygen species, leading to increased hydrogen peroxide production in rat cerebellum, and decreased GSH concentrations. Although the role of homocitrulline in depression has not been reported. However, growing data highlight

the association between major depressive disorder (MDD) and dysregulation of redox balance. This dysregulation is characterized by elevated oxidative activity and compromised antioxidant defense mechanisms. Oxidative stress disorder in depression causes an increase in brain reactive oxygen species (ROS) [55], and a decrease in the activity of the antioxidant enzyme GSH-Px [56], resulting in a decrease in the volume of the hippocampus and prefrontal cortex [47]. In our study, the concentration of homocitrulline in the model group increased significantly and decreased significantly after the intervention of BR-PRA. Furthermore, cortical differential metabolites enriched 11 metabolic pathways, including the pentose phosphate pathway, fructose and mannose metabolism, purine metabolism, etc. The pentose phosphate pathway, with the most influential signaling (Impact>0.1, $P<0.05$), is essential for maintaining cellular redox balance [57, 58]. It converts glucose-6-phosphate into pentose, generating ribose-5-phosphate and nicotinamide adenine dinucleotide phosphate (NADPH), which are crucial for anabolic biosynthesis and redox homeostasis [59]. Abnormalities in the pentose phosphate pathway lead to the reduction of NADPH, affecting the content of GSH and weakening its antioxidant effect. Therefore, BR-PRA may regulate the concentration of homocitrulline by

regulating lysine carbamylation, thereby modulating oxidative stress status in depression.

It is known that stress enhances the activity of the hypothalamus-pituitary-adrenal (HPA) axis, leading to increased secretion of corticosteroids from the adrenal cortex. Corticosterone is often used as a biomarker for stress and depressive disorders. The hypothalamus-pituitary-adrenal axis (HPA axis) is closely related to depression [60]. Studies have demonstrated increased glucocorticoid levels [61] and decreased expression of glucocorticoid receptor (GR) in the hippocampus of individuals with depression [62]. Furthermore, intervention with glucocorticoid can induce depression and down-regulation of GR expression in the hippocampus [63, 64]. Corticosterone has been reported to induce depression [65, 66], resulting in decreased hippocampal volume and neurogenesis [63, 67]. This study found that cortical corticosterone concentration was significantly increased in the CUMS model compared to the model group, and significantly decreased after the intervention of BR-PRA. Histomorphology showed that intervention with BR-PRA reversed damage to hippocampal neuronal cells, weakening changes in the structure and complexity of neuronal dendrites in depression rats.

Previous studies have confirmed that chronic stress instigates neurotoxic processes HPA axis dysregulation, inflammation, oxidative stress, and neurotransmitter disturbances [47]. These processes interact and may contribute to the development of major depressive disorder. In this study, widely targeted metabolomics was used to explore the underlying mechanisms of depression. The findings elucidated that RA-RPA may modulate depression through its effects on the HPA axis, amino acid metabolism related to lysine and glutamate, and oxidative stress. These findings provided evidence for supporting further exploration of antidepressant efficacy and clinical use of BR-PRA. Despite its contributions, this study has several limitations that warrant consideration. Firstly, the relatively small sample size in each experimental group may compromise the statistical power, thereby affecting the reliability and generalizability of the findings. Secondly, while we have identified potential metabolite biomarkers associated with depression, the absence of direct molecular validation through targeted experiments. Future research will further investigate how RA-RPA regulates metabolic pathways and metabolites associated with depression, as well as their effects on specific enzyme receptors and signaling pathways. Additionally, the mechanisms underlying the antidepressant effects of RA-RPA will be explored from a clinical perspective.

Conclusion

This study demonstrated that BR-PRA significantly alleviated depressive-like behavior, reduced hippocampal damage, and may exert inhibitory effects on depression through multiple mechanisms, including the HPA axis, amino acid metabolism related to lysine and glutamate and oxidative stress, and modulation of oxidative stress.

Abbreviations

BR-PRA	<i>Radix Bupleuri-Radix Paeoniae Alba</i>
CUMS	Chronic unpredictable mild stress
OFT	Open field test
EMP	Elevated plus-maze test
FST	Forced swimming test
HPA axis	The hypothalamus-pituitary-adrenal axis
TCM	Traditional Chinese Medicine
BDNF	Brain-derived neurotrophic factor
QC	Quality control
SD	Sprague-Dawley
PCA	Principal component analysis
OPLS-DA	Orthogonal partial least-squares discriminant analysis
MDD	Major depressive disorder
Lys	Lysine
GSH	Glutathione
CAT	Catalase
GSH-Px	Glutathione peroxidase
ROS	Reactive oxygen species
NADPH	Nicotinamide adenine dinucleotide phosphate
GR	Glucocorticoid receptor

Supplementary Information

The online version contains supplementary material available at <https://doi.org/10.1186/s12906-025-04898-8>.

Supplementary Material 1

Acknowledgements

Special thanks to Associate Professor Yongkai Cao for English language editing.

Author contributions

KC and XC: Investigation, Formal analysis, Data Curation and Writing-Original Draft; KC and LR: Software and Visualization; QB and YC: Writing-Original Draft; DH: Resources; ZF: Conceptualization, Supervision and Writing-Review; MC: Conceptualization, Supervision, Writing-Review and Funding acquisition.

Funding

This work was supported by grants from Shenzhen Science and Technology Program (No. JCYJ 20210324122803011).

Data availability

The data analyzed during the study are available from the corresponding author on reasonable request.

Declarations

Ethical approval

The animal study was reviewed and approved by the Ethical Committee in Research Medical College of China Three Gorges University of Medical Sciences (NO: 2023010U).

Consent for publication

Not applicable.

Competing interests

The authors declare no competing interests.

Author details

¹The Second People's Hospital Affiliated to Three Gorges University, Yichang Second People's Hospital, Yichang, Hubei 443000, China

²Graduate School, Guangxi University of Chinese Medicine, Nanning, Guangxi 530001, China

³College of Medicine and Health Science of China Three Gorges University, Third-Grade Pharmacological Laboratory on Chinese Medicine Approved by State Administration of Traditional Chinese Medicine, Three Gorges University, Yichang, Hubei 443002, China

⁴Department of Neurology, Shenzhen Institute of Geriatrics, The First Affiliated Hospital of Shenzhen University, Shenzhen, Guangdong 518035, China

⁵Department of Integrated Traditional Chinese and Western Medicine, Shenzhen Institute of Geriatrics, The First Affiliated Hospital of Shenzhen University, Shenzhen, Guangdong 518035, China

Received: 7 September 2024 / Accepted: 24 April 2025

Published online: 10 May 2025

References

1. Malhi GS, Mann JJ. Depression. *Lancet*. 2018;392(10161):2299–312.
2. Lasselin J, Lekander M, Benson S, Schedlowski M, Engler H. Sick for science: experimental endotoxemia as a translational tool to develop and test new therapies for inflammation-associated depression. *Mol Psychiatry*. 2021;26(8):3672–83.
3. Barnard KD, Majidi S, Clements MA, Battelino T, Renard E, Close KL, et al. RES-CUE collaborative community: A new initiative to reduce rates of intended Self-Injury and suicide among people with diabetes. *Diabetes Technol Ther*. 2022;24(8):583–7.
4. Lu J, Xu XF, Huang YQ, Li T, Ma C, Xu GM, et al. Prevalence of depressive disorders and treatment in China: a cross-sectional epidemiological study. *Lancet Psychiatry*. 2021;8(11):981–90.
5. He MC, Feng R, Wang J, Xia SH, Wang YJ, Zhang Y. Prevention and treatment of natural products from traditional Chinese medicine in depression: potential targets and mechanisms of action. *Front Aging Neurosci*. 2022;14:950143.
6. Lv J-l, Bai Y, Lv Y-e, Chen C-c, Qin X-m, Du G-h, et al. Integrated colon Microbiome and metabolomics to elucidate the antidepressant mechanisms of the Radix Bupleuri-Radix paeoniae Alba herb pair. *Metab Brain Dis*. 2024;40(1):45.
7. Zhou Y, Li T, Zhu S, Gong W, Qin X, Du G. Study on antidepressant mechanism of Radix Bupleuri-Radix paeoniae Alba herb pair by metabolomics combined with ¹H nuclear magnetic resonance and ultra-high-performance liquid chromatography-tandem mass spectrometry detection technology. *J Pharm Pharmacol*. 2021;73(9):1262–73.
8. Cai K, Zhang J, Ran L, Hu D, Feng Z, Huang H. Research progress on antidepressant Pharmacological effects and mechanisms of bupleuri radix-paeoniae Radix Alba herb-pair. *J Practical Med*. 2024;40(04):447–52.
9. Lv S, Zhao Y, Wang L, Yu Y, Li J, Huang Y, et al. Antidepressant active components of Bupleurum Chinense DC-Paeonia lactiflora pall herb pair: Pharmacological mechanisms. *Biomed Res Int*. 2022;2022:1024693.
10. Yeung W, Chung K, Ng K, Yu Y, Ziea ET, Ng BF. A systematic review on the efficacy, safety and types of Chinese herbal medicine for depression. *J Psychiatr Res*. 2014;57:165–75.
11. Wang Y, Gao SM, Li R, Zhang M, Gao S, Yu CQ. Antidepressant-like effects of the Radix bupleuri and Radix paeoniae Alba drug pair. *Neurosci Lett*. 2016;633:14–20.
12. Li X, Hou R, Qin X, Wu Y, Wu X, Tian J, et al. Synergistic neuroprotective effect of Saikosaponin A and Albiflorin on corticosterone-induced apoptosis in PC12 cells via regulation of metabolic disorders and neuroinflammation. *Mol Biol Rep*. 2022;49(9):8801–13.
13. Li X, Qin XM, Tian JS, Gao XX, Du GH, Zhou YZ. Integrated network Pharmacology and metabolomics to dissect the combination mechanisms of Bupleurum Chinense DC-Paeonia lactiflora pall herb pair for treating depression. *J Ethnopharmacol*. 2021;264:113281.
14. Yu Z, Lu T, Zhou H, Yao L, Li P, Gao S, et al. Effect of herb pair of bupleuri Radix and paeoniae Alba Radix on single amine neurotransmitter in brain of CUMS depression model of rats. *Chin Traditional Herb Drugs*. 2016;47(16):2887–92.
15. Wang H, Zhang Y, Li H, Zeng W, Qiao M. Shuyu capsules relieve liver-qi depression by regulating ERK-CREB-BDNF signal pathway in central nervous system of rat. *Exp Ther Med*. 2017;14(5):4831–8.
16. Chen JJ, Li T, Qin XM, Du GH, Zhou YZ. Integration of Non-Targeted metabolomics and targeted quantitative analysis to elucidate the synergistic antidepressant effect of Bupleurum Chinense DC-Paeonia lactiflora pall herb pair by regulating purine metabolism. *Front Pharmacol*. 2022;13:900459.
17. Dwivedi Y. Involvement of brain-derived neurotrophic factor in late-life depression. *Am J Geriatr Psychiatry*. 2013;21(5):433–49.
18. Zhang H, Zhang S, Hu M, Chen Y, Wang W, Zhang K, et al. An integrative metabolomics and network Pharmacology method for exploring the effect and mechanism of Radix bupleuri and Radix paeoniae Alba on anti-depression. *J Pharm Biomed Anal*. 2020;189:113435.
19. Chen Y, Wang W, Fu X, Sun Y, Lv S, Liu L, et al. Investigation of the antidepressant mechanism of combined Radix bupleuri and Radix paeoniae Alba treatment using proteomics analysis of liver tissue. *J Chromatogr B Analyt Technol Biomed Life Sci*. 2021;1179:122858.
20. Kito S, Hasegawa T, Koga Y. Cerebral blood flow ratio of the dorsolateral prefrontal cortex to the ventromedial prefrontal cortex as a potential predictor of treatment response to transcranial magnetic stimulation in depression. *Brain Stimul*. 2012;5(4):547–53.
21. Jung S, Choe S, Woo H, Jeong H, An HK, Moon H, et al. Autophagic death of neural stem cells mediates chronic stress-induced decline of adult hippocampal neurogenesis and cognitive deficits. *Autophagy*. 2020;16(3):512–30.
22. Antoniuk S, Bijata M, Ponimaskin E, Włodarczyk J. Chronic unpredictable mild stress for modeling depression in rodents: Meta-analysis of model reliability. *Neurosci Biobehav Rev*. 2019;99:101–16.
23. Marsden WN. Synaptic plasticity in depression: molecular, cellular and functional correlates. *Prog Neuropsychopharmacol Biol Psychiatry*. 2013;43:168–84.
24. Qiao H, Li M-X, Xu C, Chen H-B, An S-C, Ma X-M. Dendritic spines in depression: what we learned from animal models. *Neural Plast*. 2016;2016:8056370.
25. Yang J, Jin W, Liu D, Zhong Q, Zhou T. Enhanced pseudotargeted analysis using a segment data dependent acquisition strategy by liquid chromatography-tandem mass spectrometry for a metabolomics study of liquiritin in the treatment of depression. *J Sep Sci*. 2020;43(11):2088–96.
26. Liu D, Yang J, Jin W, Zhong Q, Zhou T. A high coverage pseudotargeted lipidomics method based on three-phase liquid extraction and segment data-dependent acquisition using UHPLC-MS/MS with application to a study of depression rats. *Anal Bioanal Chem*. 2021;413(15):3975–86.
27. Fang S, Dong L, Liu L, Guo J, Zhao L, Zhang J, et al. HERB: a high-throughput experiment- and reference-guided database of traditional Chinese medicine. *Nucleic Acids Res*. 2021;49(D1):D1197–206.
28. Ru J, Li P, Wang J, Zhou W, Li B, Huang C, et al. TCMSP: a database of systems Pharmacology for drug discovery from herbal medicines. *J Cheminform*. 2014;6:13.
29. Bu Q, Zhang J, Guo X, Feng Y, Yan H, Cheng W, et al. The antidepressant effects and serum metabolomics of bifid triple viable capsule in a rat model of chronic unpredictable mild stress. *Front Nutr*. 2022;9:947697.
30. Huang CY, Zhang FC, Li P, Song C, Low-Dose. IL-2 attenuated depression-like behaviors and pathological changes through restoring the balances between IL-6 and TGF-beta and between Th17 and Treg in a chronic Stress-Induced mouse model of depression. *Int J Mol Sci*. 2022;23(22):13856.
31. Underwood W, Anthony R. AVMA guidelines for the euthanasia of animals: 2020 edition. Am Veterinary Med Association Publishing. 2020;2013(30):2020–1.
32. De Souza LP, Alseekh S, Brotman Y, Fernie AR. Network-based strategies in metabolomics data analysis and interpretation: from molecular networking to biological interpretation. *Expert Rev Proteomics*. 2020;17(4):243–55.
33. Battle S, Gogonea V, Willard B, Wang ZN, Fu XM, Huang Y, et al. The pattern of Apolipoprotein A-I lysine carbamylation reflects its lipidation state and the chemical environment within human atherosclerotic aorta. *J Biol Chem*. 2022;298(4):101832.
34. Matthews DE. Review of lysine metabolism with a focus on humans. *J Nutr*. 2020;150(Suppl 1):S2548–55.
35. Cinelli MA, Do HT, Miley GP, Silverman RB. Inducible nitric oxide synthase: regulation, structure, and inhibition. *Med Res Rev*. 2020;40(1):158–89.
36. Papes F, Surpili MJ, Langone F, Trigo JR, Arruda P. The essential amino acid lysine acts as precursor of glutamate in the mammalian central nervous system. *FEBS Lett*. 2001;488(1–2):34–8.
37. Smriga M, Torii K. L-Lysine acts like a partial serotonin receptor 4 antagonist and inhibits serotonin-mediated intestinal pathologies and anxiety in rats. *Proc Natl Acad Sci U S A*. 2003;100(26):15370–5.

38. Srinongkote S, Smriga M, Nakagawa K, Toride Y. A diet fortified with L-lysine and L-arginine reduces plasma cortisol and blocks anxiogenic response to transportation in pigs. *Nutr Neurosci*. 2003;6(5):283–9.
39. Jezova D, Makatsori A, Smriga M, Morinaga Y, Duncko R. Subchronic treatment with amino acid mixture of L-lysine and L-arginine modifies neuroendocrine activation during psychosocial stress in subjects with high trait anxiety. *Nutr Neurosci*. 2005;8(3):155–60.
40. Smriga M, Ando T, Akutsu M, Furukawa Y, Miwa K, Morinaga Y. Oral treatment with L-lysine and L-arginine reduces anxiety and basal cortisol levels in healthy humans. *Biomed Res*. 2007;28(2):85–90.
41. Chang YF, Gao XM. L-lysine is a barbiturate-like anticonvulsant and modulator of the benzodiazepine receptor. *Neurochem Res*. 1995;20(8):931–7.
42. Wellendorph P, Hansen KB, Balsgaard A, Greenwood JR, Egebjerg J, Brauner-Osborne H. Deorphanization of GPRC6A: a promiscuous L-alpha-amino acid receptor with preference for basic amino acids. *Mol Pharmacol*. 2005;67(3):589–97.
43. Smriga M, Murakami H, Mori M, Torii K. Effects of L-lysine deficient diet on the hypothalamic interstitial norepinephrine and diet-induced thermogenesis in rats in vivo. *BioFactors*. 2000;12(1–4):137–42.
44. Smriga M, Kameishi M, Uneyama H, Torii K. Dietary L-lysine deficiency increases stress-induced anxiety and fecal excretion in rats. *J Nutr*. 2002;132(12):3744–6.
45. Kondoh T, Kameishi M, Mallick HN, Ono T, Torii K. Lysine and arginine reduce the effects of cerebral ischemic insults and inhibit glutamate-induced neuronal activity in rats. *Front Integr Neurosci*. 2010;4:18.
46. Banasr M, Chowdhury GM, Terwilliger R, Newton SS, Duman RS, Behar KL, et al. Glial pathology in an animal model of depression: reversal of stress-induced cellular, metabolic and behavioral deficits by the glutamate-modulating drug riluzole. *Mol Psychiatry*. 2010;15(5):501–11.
47. Belleau EL, Treadway MT, Pizzagalli DA. The impact of stress and major depressive disorder on hippocampal and medial prefrontal cortex morphology. *Biol Psychiatry*. 2019;85(6):443–53.
48. Hasler G, van der Veen JW, Tuminis T, Meyers N, Shen J, Drevets WC. Reduced prefrontal glutamate/glutamine and gamma-aminobutyric acid levels in major depression determined using proton magnetic resonance spectroscopy. *Arch Gen Psychiatry*. 2007;64(2):193–200.
49. Tapias A, Wang ZQ. Lysine acetylation and deacetylation in brain development and neuropathies. *Genomics Proteom Bioinf*. 2017;15(1):19–36.
50. Gavin DP, Kartan S, Chase K, Jayaraman S, Sharma RP. Histone deacetylase inhibitors and candidate gene expression: an in vivo and in vitro approach to studying chromatin remodeling in a clinical population. *J Psychiatr Res*. 2009;43(9):870–6.
51. Machado-Vieira R, Ibrahim L, Zarate CA. Jr. Histone deacetylases and mood disorders: epigenetic programming in gene-environment interactions. *CNS Neurosci Ther*. 2011;17(6):699–704.
52. Vavakova M, Durackova Z, Trebatická J. Markers of oxidative stress and neuroprogression in depression disorder. *Oxid Med Cell Longev*. 2015;2015:898393.
53. Viegas CM, Tonin AM, Zanatta A, Seminotti B, Busanello EN, Fernandes CG, et al. Impairment of brain redox homeostasis caused by the major metabolites accumulating in hyperornithinemia-hyperammonemia-homocitrullinuria syndrome in vivo. *Metab Brain Dis*. 2012;27(4):521–30.
54. Zanatta A, Viegas CM, Tonin AM, Busanello EN, Grings M, Moura AP, et al. Disturbance of redox homeostasis by ornithine and homocitrulline in rat cerebellum: a possible mechanism of cerebellar dysfunction in HHH syndrome. *Life Sci*. 2013;93(4):161–8.
55. Zou T, Zhang J, Liu Y, Zhang Y, Sugimoto K, Mei C. Antidepressant-Like effect of Geniposide in mice exposed to a chronic mild stress involves the microRNA-298-5p-Mediated Nox1. *Front Mol Neurosci*. 2020;13:131.
56. Michel TM, Pulschen D, Thome J. The role of oxidative stress in depressive disorders. *Curr Pharm Des*. 2012;18(36):5890–9.
57. Chung YE, Chen HC, Chou HL, Chen IM, Lee MS, Chuang LC, et al. Exploration of microbiota targets for major depressive disorder and mood related traits. *J Psychiatr Res*. 2019;111:74–82.
58. Ozaslan MS, Balci N, Demir Y, Gurbuz M, Kufrevioglu OI. Inhibition effects of some antidepressant drugs on Pentose phosphate pathway enzymes. *Environ Toxicol Pharmacol*. 2019;72:103244.
59. Tu D, Gao Y, Yang R, Guan T, Hong JS, Gao HM. The Pentose phosphate pathway regulates chronic neuroinflammation and dopaminergic neurodegeneration. *J Neuroinflammation*. 2019;16(1):255.
60. Pariante CM, Lightman SL. The HPA axis in major depression: classical theories and new developments. *Trends Neurosci*. 2008;31(9):464–8.
61. Zhou W, Ye S, Luo R, Wu LM, Wang W. Inhibition of acid-sensing ion channels reduces the hypothalamus-pituitary-adrenal axis activity and ameliorates depression-like behavior in rats. *RSC Adv*. 2019;9(16):8707–13.
62. D'Alessio L, Mesarosova L, Anink JJ, Kochen S, Solis P, Oddo S, et al. Reduced expression of the glucocorticoid receptor in the hippocampus of patients with drug-resistant Temporal lobe epilepsy and comorbid depression. *Epilepsia*. 2020;61(8):1595–605.
63. Goshen I, Kreisel T, Ben-Menachem-Zidon O, Licht T, Weidenfeld J, Ben-Hur T, et al. Brain interleukin-1 mediates chronic stress-induced depression in mice via adrenocortical activation and hippocampal neurogenesis suppression. *Mol Psychiatry*. 2008;13(7):717–28.
64. Kajiyama Y, Iijima Y, Chiba S, Furuta M, Ninomiya M, Izumi A, et al. Prednisolone causes anxiety- and depression-like behaviors and altered expression of apoptotic genes in mice hippocampus. *Prog Neuropsychopharmacol Biol Psychiatry*. 2010;34(1):159–65.
65. David DJ, Samuels BA, Rainer Q, Wang JW, Marsteller D, Mendez I, et al. Neurogenesis-dependent and -independent effects of Fluoxetine in an animal model of anxiety/depression. *Neuron*. 2009;62(4):479–93.
66. Zhao Y, Ma R, Shen J, Su H, Xing D, Du L. A mouse model of depression induced by repeated corticosterone injections. *Eur J Pharmacol*. 2008;581(1–2):113–20.
67. Chen L, Wang X, Lin ZX, Dai JG, Huang YF, Zhao YN. Preventive effects of ginseng total saponins on chronic Corticosterone-Induced impairment in astrocyte structural plasticity and hippocampal atrophy. *Phytother Res*. 2017;31(9):1341–8.

Publisher's note

Springer Nature remains neutral with regard to jurisdictional claims in published maps and institutional affiliations.